Environmental Science Processes & Impacts

ROYAL SOCIETY OF CHEMISTRY

PAPER

View Article Online
View Journal | View Issue

Cite this: *Environ. Sci.: Processes Impacts*, 2022, **24**, 1212

Early and late cyanobacterial bloomers in a shallow, eutrophic lake†

Kristin J. Painter, *[a] Jason J. Venkiteswaran, [b] Dana F. Simon, [c] Sung Vo Duy,[c] Sébastien Sauvé [c] and Helen M. Baulch [a]

Cyanobacterial blooms present challenges for water treatment, especially in regions like the Canadian prairies where poor water quality intensifies water treatment issues. Buoyant cyanobacteria that resist sedimentation present a challenge as water treatment operators attempt to balance pre-treatment and toxic disinfection by-products. Here, we used microscopy to identify and describe the succession of cyanobacterial species in Buffalo Pound Lake, a key drinking water supply. We used indicator species analysis to identify temporal grouping structures throughout two sampling seasons from May to October 2018 and 2019. Our findings highlight two key cyanobacterial bloom phases – a mid-summer diazotrophic bloom of *Dolichospermum* spp. and an autumn *Planktothrix agardhii* bloom. *Dolichospermum crassa* and *Woronichinia compacta* served as indicators of the mid-summer and autumn bloom phases, respectively. Different cyanobacterial metabolites were associated with the distinct bloom phases in both years: toxic microcystins were associated with the mid-summer *Dolichospermum* bloom and some newly monitored cyanopeptides (anabaenopeptin A and B) with the autumn *Planktothrix* bloom. Despite forming a significant proportion of the autumn phytoplankton biomass (>60%), the *Planktothrix* bloom had previously not been detected by sensor or laboratory-derived chlorophyll-*a*. Our results demonstrate the power of targeted taxonomic identification of key species as a tool for managers of bloom-prone systems. Moreover, we describe an autumn *Planktothrix agardhii* bloom that has the potential to disrupt water treatment due to its evasion of detection. Our findings highlight the importance of identifying this autumn bloom given the expectation that warmer temperatures and a longer ice-free season will become the norm.

Received 23rd February 2022
Accepted 5th July 2022

DOI: 10.1039/d2em00078d

rsc.li/espi

Environmental significance

Cyanobacterial blooms threaten water supplies, especially in the vast, yet understudied prairie regions where pressures on water security mean water quality is often considered secondarily to water quantity. Understanding the structure, composition, and metabolites of cyanobacterial communities is essential for water treatment operators who must balance risks of high cyanobacterial biomass with those of toxic disinfection by-products in systems with inherently poor and declining water quality. Our work demonstrated two cyanobacterial bloom periods: a toxic mid-summer bloom of nitrogen-fixers, and a secondary bloom of the genera *Planktothrix* that, despite in-lake monitoring with high-frequency sensors, was previously undetected. This autumn bloom highlights a knowledge gap that must be considered by researchers and practitioners as open-water seasons lengthen with climate warming.

Introduction

Cyanobacterial bloom frequency and severity is expected to expand globally[1–3] as the effects of eutrophication[4] and climate change[5,6] become more profound. Especially at risk are the shallow, eutrophic lakes of the North American prairies.[7,8] Here, the cumulative impacts of climate change and intensive watershed land use are contributing to increasingly severe cyanobacterial blooms.[8,9] For example, extensive agriculture and accelerated runoff-driven nutrient transport from land-to-lake have been linked to the rapid eutrophication and subsequent expansion of toxin-producing cyanobacterial blooms in Lake Winnipeg.[9–11] Warming surface water temperatures and a longer ice-free season appear to be associated with increasingly potent concentrations of toxic microcystins in shallow, polymictic prairie lakes.[12] Moreover, evidence from sediment cores suggests the abundance of toxin-producing cyanobacterial species (*e.g.*, *Dolichospermum* spp.) may be increasing in some prairie lakes.[13] Despite these pressures in the prairies, many

[a]*School of Environment and Sustainability, Global Institute for Water Security, University of Saskatchewan, Saskatoon, SK S7N 5C8, Canada. E-mail: kristin.painter@usask.ca*

[b]*Department of Geography and Environmental Studies, Wilfrid Laurier University, Waterloo, ON N2L 3C5, Canada*

[c]*Department of Chemistry, Université de Montréal, Montréal, QC H2V 0B3, Canada*

† Electronic supplementary information (ESI) available. See https://doi.org/10.1039/d2em00078d

waterbodies provide key ecosystem services including critical drinking water supplies. Therefore, understanding algal community composition in bloom-afflicted lakes is critical for effective management.

The impacts of cyanobacterial species are of particular concern due to their ability to produce toxic metabolites, thereby presenting potential human health risks. Shallow prairie lakes appear to be especially susceptible to toxin-producing cyanobacterial blooms, for example, Loewen *et al.*[14] found a negative correlation between depth and toxin production in Alberta lakes, a link they attributed to the polymictic nature of many shallow prairie lakes whereby frequent mixing provides phosphorus (P) enrichment from deeper waters to phytoplankton. Plentiful P and limited inflow of nitrogen (N) from the watershed throughout the summer months in many prairie systems favours the growth of N-fixing genera such as *Dolichospermum* and *Aphanizomenon* known to produce toxins.[7,15] Shallow prairie lakes are also more susceptible to warming,[16] a driver that has also been linked to blooms[17] thus concerns also remain about non-diazotrophic species (*e.g.*, *Planktothrix*, *Microcystis*) that have the potential to proliferate and contribute to toxin risk. Consequently, improved understanding of the species and associated toxins is needed to guide more in-depth analysis and management of these systems.

The physicochemical properties of many toxin-producing species can also impede their removal during drinking water treatment. For example, filamentous species (*e.g.*, *Aphanizomenon* and *Planktothrix* spp.) can foul filtering infrastructure while others, *e.g.*, *Microcystis* genera, are resistant to coagulation making their removal during sedimentation processes challenging.[18–20] High phytoplankton biomass can be particularly difficult to deal with for water 2treatment operators who must manage particulate loads and balance the use of disinfection processes such as pre-chlorination with the risk of toxic disinfection by-products. When present in large quantities, phytoplankton biomass may contribute to rising floc – aggregates of solid material that cannot be effectively overcome by coagulation (and subsequent sedimentation) alone. Pre-chlorination at the outset of the treatment process may reduce problems associated with bloom impacts on processes such as rising flocs by killing buoyant algae,[21] however, when chlorine reacts with naturally occurring organic matter, toxic trihalomethanes (THMs) are produced.[22] Operators must meet THM limits while maintaining adequate drinking water supplies. Moreover, some toxin producing species may persist after oxidation whether they were dominant species or not,[23] adding to the complexity of managing bloom-prone water supplies.

Though cyanobacterial blooms are common in shallow prairie lakes, the intra- and interannual variation inherent to the prairie region contributes to the difficulty in predicting the severity of blooms.[24] Treatment operations may need to be altered quickly in response and the availability of additional tools with high ease-of-use to managers is imperative. Non-specific indicators of algal biomass, such as chlorophyll-*a* (chl-*a*), have enabled managers to establish links between in-lake algal blooms and water treatment issues;[25,26] however, such measurements provide limited information about the organisms responsible for treatment disruptions. Operators of municipal water supplies in Canada also frequently employ routine in-house microscopy to estimate cyanobacterial phytoplankton cell counts as part of source water monitoring.[27] Thus, additional identification of the presence of key species indicative of cyanobacterial blooms could provide managers with an early indicator of those blooms that have the potential to affect water treatment operations, something not possible with non-specific biomass indicators.

Here, we examine the structure of the taxonomically identified algal community throughout two ice-free seasons in a shallow, polymictic prairie lake that serves as a major drinking water supply. We use a combination of clustering, indicator species analysis, and ordination to describe the succession of algal community abundance over time and identify potential indicator species common across years and time periods. We also provide new information about the types and concentrations of cyanotoxins present and describe their correlation to the cyanobacterial community. Finally, we contrast the common algal biomass indicator chl-*a* and the findings of our taxonomic analysis. The objective of this paper is to identify the seasonal evolution of harmful cyanobacteria and their toxins in a crucial drinking water supply and demonstrate the utility of targeted taxonomic identification of key species as a tool for managers.

Methods

Site description

Buffalo Pound Lake is a shallow, polymictic prairie reservoir located in Saskatchewan, Canada (Fig. 1). The lake is approximately 29 km in length, 1.0 km wide and has an average depth of approximately 3.0 m (maximum depth: 5.8 m). The lake is fed primarily by upstream Lake Diefenbaker, a large mesotrophic reservoir, *via* the Qu'Appelle River. In addition to water from this upstream reservoir, the lake also receives inflow from the local catchment which has a gross drainage area of 3393 km^2 and is predominantly (>70%) agricultural. The effective drainage area (*i.e.*, the area contributing runoff in a median year) is approximately 38% of the gross drainage area (J-M. Davies, Water Security Agency, pers. comm). Local runoff occurs predominantly during the snowmelt period, as is common for most prairie systems.[28] Buffalo Pound Lake's outflow has been controlled since 1939 to regulate water levels for direct and downstream use.[29] Water level is tightly regulated, varying only a few centimeters each year.[30] Water residence time is short (typically <one year); however, it can vary more than five-fold, depending on runoff, precipitation, and management decisions.[31]

Buffalo Pound Lake serves as an important water supply in a relatively water scarce, semi-arid to subhumid region where water quality is affected by eutrophication and annual cyanobacterial blooms.[8,34] The lake is an important drinking water source, supplying drinking water to a quarter of the province's population, approximately 260 000 people, in addition to substantive water withdrawals to support industry including local mines. The annual range of known concentrations for chl-*a* is approx. 5.0 to 170 μg L^{-1} and <2.0 to 340 μg L^{-1} for total P.[35] Additionally, dissolved organic matter (DOM) in Buffalo Pound is

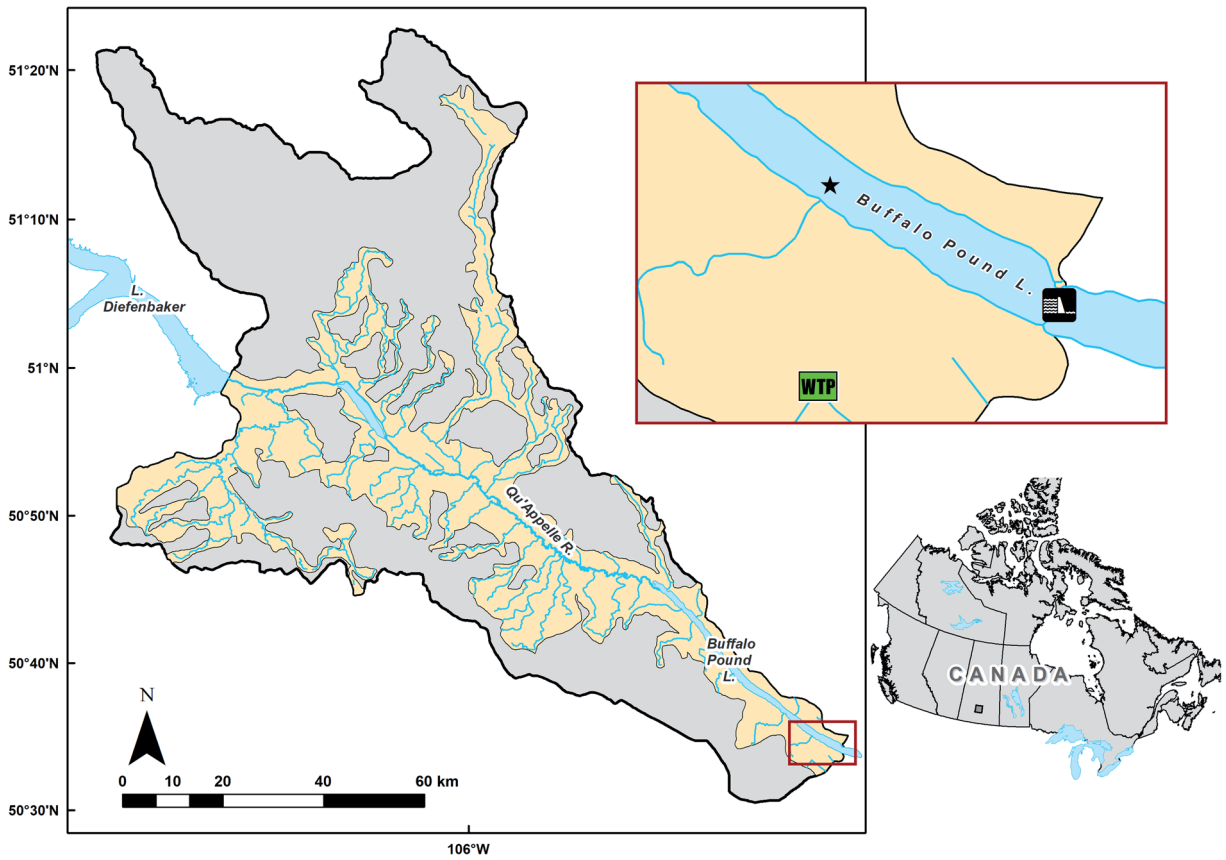

Fig. 1 Map of Buffalo Pound Lake, Saskatchewan, Canada, and its gross (grey) and effective (yellow) drainage area, including upstream Lake Diefenbaker. The inset map (red outline) indicates the location of the Buffalo Pound Water Treatment Plant (green WTP symbol) and the sampling site (star symbol; 50°35′8.8″ N, 105°23′0.24″ W) near its intakes. The Buffalo Pound Dam, which controls lake water level, is shown at the southeast end of the lake (black and white dam symbol). Geospatial data used to create this map was downloaded from CanVec[32] and ArcGIS Online.[33]

relatively high for a drinking water source. The poor source water quality creates major challenges for water treatment, for example in 2015 water shortages occurred resulting from early bloom conditions co-occurring with extreme stratification.[36] The drinking water treatment plant uses a process which includes pre-chlorination, coagulation (with alum or polyaluminum chloride), flocculation, clarification, filtration, and then final disinfection before the water is distributed to the cities of Moose Jaw and Regina, Saskatchewan. Cascade degasification and granular activated carbon is used seasonally, near the start and end of the process train respectively while powdered activated carbon is used on an as-needed basis to due reduce excess taste and odour compounds. While pre-chlorination was briefly discontinued to manage disinfection by-products (THMs); issues with flocculation and clarification have occurred periodically associated with bloom periods, and vigilance is required to manage the concurrent issues of blooms of buoyant cyanobacteria, transient lake stratification, and high DOM.

Sample collection and analysis

Samples were collected approximately weekly during the ice-free season from May to October 2018 ($n = 25$) and 2019 ($n = 17$) from a monitoring site located near the Buffalo Pound Water Treatment Plant intake (50°35′8.8″ N, 105°23′0.24″ W; Fig. 1). On-site water temperature was recorded at 0.2 m depth intervals using a YSI (6500 series) multi-probe sonde (YSI, Ohio, USA; Fig. S1†). Discrete grab samples were collected at 0.8 m using a Van Dorn sampler and partitioned for phytoplankton enumeration, cyanobacterial metabolites, and chl-*a*. Samples for chl-*a* were collected into acid-washed opaque high density polyethylene bottles and samples for cyanobacterial metabolites were collected into polyethylene terephthalate glycol (PETG) amber bottles.

Water samples collected for intra- and extracellular cyanobacterial metabolites were filtered (100 ml) on the day of collection through a 0.45 μm hydrophilic polypropylene (GHP) membrane filter,[37] without adjusting sample pH (mean pH = 8.29 ± 0.31 in 2018 and 8.64 ± 0.37 in 2019). Filters were enclosed in a Petri dish and frozen until time of analysis for intracellular metabolites. The filtrate phase was collected in PETG amber bottles for dissolved (extracellular) toxin analysis and frozen at −20 °C until analysis.[38] Samples were shipped to Université de Montréal in Montréal, Canada for analysis of total microcystins and 17 cyanobacterial metabolites (see also Texts S1–S2 and Table S1†). The analysis of filters proceeded as follows. Following addition of 5 mL of 90 : 10 MeOH/water, the

filters were ultrasonicated (15 min), centrifuged (10 min, 6000 rpm), and the liquid phase transferred to a fresh extraction tube. The extraction process was repeated once (two extraction cycles), and the combined solution evaporated to dryness prior to reconstitution in 5 mL of HPLC-water. Following filtration through GHP and addition of internal standards, aqueous solutions were analyzed by on-line solid-phase extraction (SPE) ultra-high-performance liquid chromatography (UHPLC) tandem mass spectrometry (MS/MS) or high-resolution mass spectrometry (HRMS), using the same instrumental methods as for dissolved samples.

For total microcystins, a 5 mL aliquot of water was filtered through a GHP; a sub-aliquot was amended with MMPB-d3 prior to permanganate oxidation (to generate the 2-methyl-3-methoxy-4-phenylbutyric acid (MMPB) moiety), and subsequently analyzed by on-line SPE – UHPLC-MS/MS (Thermo TSQ Quantiva).[39,40] For individual cyanotoxins (anabaenopeptin A, anabaenopeptin B, anatoxin-a, homoanatoxin-a, cylindrospermopsin, and microcystins -dm-RR, -RR, -YR, -HtyR, -LR, -dm-LR, -HilR, -WR, -LA, -LY, -LF, and -LW), a 5 mL aliquot of water was filtered through a GHP; a sub-aliquot was amended with an internal standard mix and analyzed by on-line SPE – UHPLC-HRMS (Thermo Orbitrap Q-Exactive).[37] Matrix-matched calibration (additions to blank lake water, calibration range of LOQ-1000 ng L^{-1}) with internal standard correction was used to quantify cyanotoxins, with accuracies within 81–113%.[37] All samples were analyzed in duplicate. If specific samples surpassed the high-end calibration level, a new sample preparation was performed by using a diluted aliquot of the sample for analysis; concentration in the initial sample was then derived applying the dilution factor.

Phytoplankton samples were preserved with Lugol's iodine upon collection, concentrated, and shipped to Plankton R Us in Winnipeg, Canada for enumeration and identification by D. L. Findlay. Larsen *et al.*[41] provide a detailed description of enumeration methods. In brief, samples were enumerated and identified to the species level using an inverted microscope following the methods described in Findlay and Kling.[42] In addition to viable vegetative cells (*i.e.*, with intact chloroplast), cyanobacterial heterocytes were also enumerated if present. Cell counts were converted to wet weight biomass by approximating cell volume using measurements of individual cells and applying the geometric formula best fitted to the shape of the cell per Vollenweider.[43]

Chl-*a* samples were analyzed at the Saskatchewan Water Chemistry and Ecology laboratory at the University of Saskatchewan Global Institute for Water Security in Saskatoon, Canada. Samples were prepared by filtering 100–300 ml of sampled lake water through glass fiber filters (GF/Fs) and freezing filters until analysis. Prior to analysis, GF/Fs were digested in 95% ethanol for 24 hours[44] and absorbance of the resulting solution was measured at 649, 655 and 750 nm on a Shimadzu UV-1601PC spectrophotometer.

Statistical analysis

All statistical analyses were conducted using R statistical software.[45] To better understand patterns in species composition throughout the sampling season, we classified the phytoplankton data from each year into distinct groups. To identify clusters, K-means partitioning was performed on Hellinger standardized[46] phytoplankton community abundance data (*e.g.*, biomass) with two to five partitions. Then, indicator species analysis was performed on the clustered data sets to identify the ideal number of groupings as described by De Cáceres *et al.*[47] The multipatt function in the indicspecies R package[48] was used to calculate group-equalized indicator values (IndVals) for each species using untransformed data. IndVals consist of a probability metric and a frequency metric which indicate the likelihood of group membership given detection of the indicator species, and the frequency of species occurrence within a given group, respectively.[47,49] IndVals vary between 0.0 and 1.0, with strength of species association with a particular group increasing from 0.0 (no association) to 1.0 (strong association). A permutation test is used to detect significance of the association between indicators and groups ($\alpha = 0.05$). The number of partitions from two to five with the highest number of significant indicator species was considered the best grouping.

IndVals were calculated in two ways, first considering only the associations between species and each group, and second considering possible associations between species and single groups plus group combinations. Group combinations were included because indicator species associated to two or more groups allow for interpretation of similarity between groupings because they characterize a higher-level grouping structure than would otherwise be indicated by single groups only.[47]

Prior to analysis of individual intracellular cyanotoxin data, values below LOD were replaced with zero. In the rare instance that values ($n = 3$ occurrences for individual MC congeners) were greater than LOD but less than level of quantification (LOQ), they were replaced with their respective LOQs (see Table S1†). A squareroot transformation was then applied to the dataset to reduce skewness and the envfit function in R package vegan[50] was used to fit toxin vectors onto a non-metric multidimensional scaling (NMDS) ordination of the cyanobacterial phytoplankton community using permutation tests. Finally, non-parametric Spearman rank correlations (r_s) were used to assess relationships between the biomass of individual cyanobacterial species and the most predominant toxin concentrations (total microcystins, anabaenopeptins A and B).

Results

Community composition

The phytoplankton community present in Buffalo Pound Lake consisted of 73 species in the 2018 sampling season and 56 in the 2019 sampling season. In both years, partitioning the community into three groups resulted in the highest number of significant indicator species when only single groups were considered ($n = 21$ in 2018 and $n = 20$ in 2019). When group combinations were considered, the highest number of significant indicator species in 2019 was again associated with three groups ($n = 19$). However, the 2018 data had a higher number of significant indicator species when the community was partitioned into four groups ($n = 20$) with the second-highest

number attributed to three groups ($n = 16$). However, with four partitions, more than half of the species (11) were associated with a combination grouping of three groups (*i.e.*, species that were present for much of the year) therefore we determined partitioning the 2018 phytoplankton community into three groups to be a more accurate depiction of the change in overall community structure through time.

Despite differences in the overall number of species detected, partitioning placed the phytoplankton community into three similar temporally defined groups in both years: Group A consisting largely of early-season algal species; Group B contained the early to mid-summer blooming diazotrophic cyanophyte species; and Group C was dominated by the late-season non-diazotrophic cyanophyte species (Fig. 2). In 2018 (Fig. 2a), Group A contained only the first two sampling days (late May and early June) and was dominated by chrysophytes (73% of Group A biomass), especially *Dinobryon sertularia* (43%) and *Chrysochromulina parva* (11%). Cyanophytes accounted for 75% and 70% of 2018 Group B and C biomass, respectively. Group B spanned from mid-June to mid-July (DOY 170 to 193) and also included August 8th (DOY 220). Three cyanophyte species accounted for much of the biomass: *Dolichospermum flos-aquae* and *D. crassa* accounted for 44% of Group B biomass while *Planktothrix agardhii* contributed 29%. Group C, which included mid-July to mid-September (DOY 197 to 260 but excluding 220), was associated with a shift in the cyanophyte community from *Dolichospermum* spp. dominant to *P. agardhii* dominant. *P. agardhii* contributed 63% of the total biomass in Group C while the *Dolichospermum* species contributed less than 5% collectively.

In 2019 (Fig. 2b), Group A spanned the first four sampling days, extending later into June (DOY 170) than in 2018. Cryptophytes and chrysophytes accounted for nearly half of the Group A biomass in 2019 (31% and 16% respectively), however, cyanophytes contributed a much larger proportion (43%) than was observed for Group A in 2018 (5%), largely due to *D. flos-aquae* (41% of Group A biomass). Like in 2018, in 2019 cyanophytes accounted for much of the biomass for the remainder of

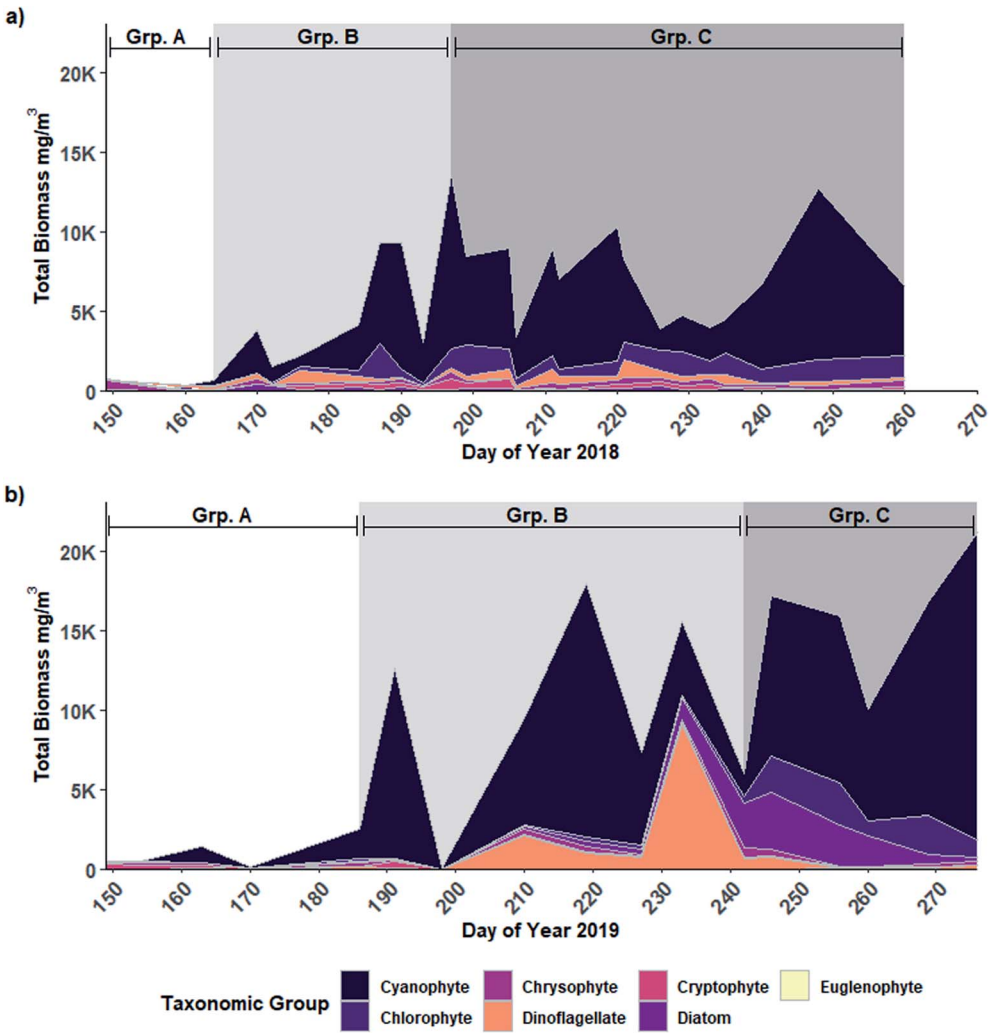

Fig. 2 Abundance (measured as biomass in mg m^{-3}) of phytoplankton taxonomic groups from samples collected in (a) 2018 and (b) 2019 from 0.8 m depth in Buffalo Pound Lake, Saskatchewan. Shading indicates grouping based on K-means partitioning and indicator species analysis: Group A ("Grp. A"), Group B ("Grp. B"), and Group C ("Grp. C").

the year: 68% of Group B biomass and 74% of Group C biomass. Group B spanned from early July to late August (DOY 186 to 242) and was again dominated by diazotrophs including *D. crassa* (33%), *D. flos-aquae* (16%) and *Aphanizomenon flos-aquae* (14%). Unlike 2018, *P. agardhii* only accounted for 2% of Group B biomass in 2019; however, it again became the wholly dominant species in Group C (DOY 264 to 276) contributing 63% to 88% of the total biomass from mid-September to October.

Individual indicator species were also similar between years. For example, the chrysophyte species *Dinobryon sertularia* was a significant Group A indicator in both 2018 (IndVal = 0.963, $p = 0.001$) and 2019 (IndVal = 1.00, $p = 0.001$). The diazotrophs *D. crassa* (IndVal = 0.931, $p = 0.001$) and *A. flos-aquae* (IndVal = 0.997, $p = 0.001$) were significant indicator species of Group B in 2018 and 2019, respectively. *D. crassa* was an indicator of the combination of Group A and B in 2019 (IndVal = 1.00, $p = 0.001$). The cyanophyte species *Woronichinia compacta* was a common Group C indicator species in both years (IndVal > 0.960, $p = 0.001$). Additionally, non-diazotrophic cyanophytes *P. agardhii* (IndVal = 0.990, $p = 0.001$) and *Merismopedia tenuissima* were Group C indicators (IndVal = 0.834, $p = 0.017$) in 2019 while *P. agardhii* was an indicator of the Group B and C combination in 2018 (IndVal = 1.00, $p = 0.009$). A complete list of indicator species by group and group combination and their indicator values can be found in Table S2.†

The seasonal patterns apparent in both years indicate a shift from a community dominated by diazotrophic species (*i.e.*, Group B) to non-diazotrophic species (*i.e.*, Group C) composed largely of *Dolichospermum* spp. and *Planktothrix* spp. (Fig. 3a and b and S1†). N-fixation during the diazotrophic period was demonstrated by the presence of heterocytes belonging to diazotrophic taxa (*sensu* Boyer 2021) including *D. crassa*, *D. flos-aquae*, and *D. solitaria* in 2018 (Fig. 3c) and *D. crassa*, *D. flos-aquae* and *Aphanizomenon flos-aquae* in 2019 (Fig. 3d). The majority of heterocyte abundance was contributed by *D. crassa* and *D. flos-aquae* (Fig. 3c and d). Both *Dolichospermum* spp. and heterocyte biomass was greater in 2019 (max = 11 848 and 942 mg m^{-3}, respectively) than 2018 (max = 4400 and 357 mg m^{-3}, respectively), particularly that of *D. crassa*.

Cyanotoxins

Total microcystins and a suite of 17 cyanometabolites measured in intracellular and extracellular samples in 2018 and 2019 (Table S1;† Fig. 4) followed a similar seasonal pattern but differed in concentration. In both years, a seasonal progression was observed from undetectable levels in the early spring to a dominance of microcystin congeners in intracellular samples in the mid-summer coinciding with peak N-fixer biomass (Group B). Microcystins were largely replaced by anabaenopeptins in the late summer and early autumn with peak

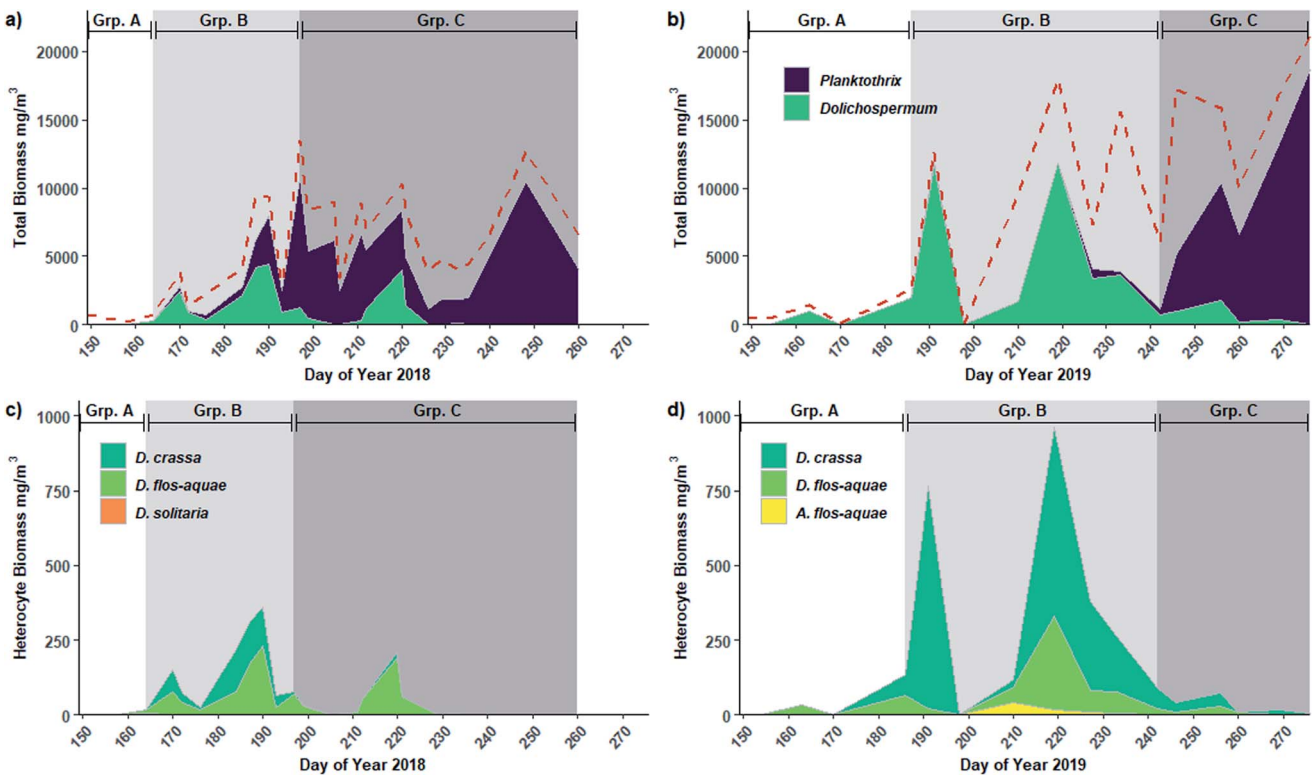

Fig. 3 Mid-summer cyanobacterial blooms dominated by nitrogen fixing *Dolichospermum* spp. (green) give way to non-diazotrophic *Planktothrix agardhii* (purple) dominated communities in Buffalo Pound Lake in 2018 (a) and 2019 (b). Dashed red line indicates total phytoplankton biomass. Nitrogen fixation is inferred from the presence of heterocytes coinciding with *Dolichospermum* spp. dominated communities in 2018 (c) and 2019 (d). Shading indicates grouping based on K-means partitioning and indicator species analysis: Group A ("Grp. A"), Group B ("Grp. B"), and Group C ("Grp. C").

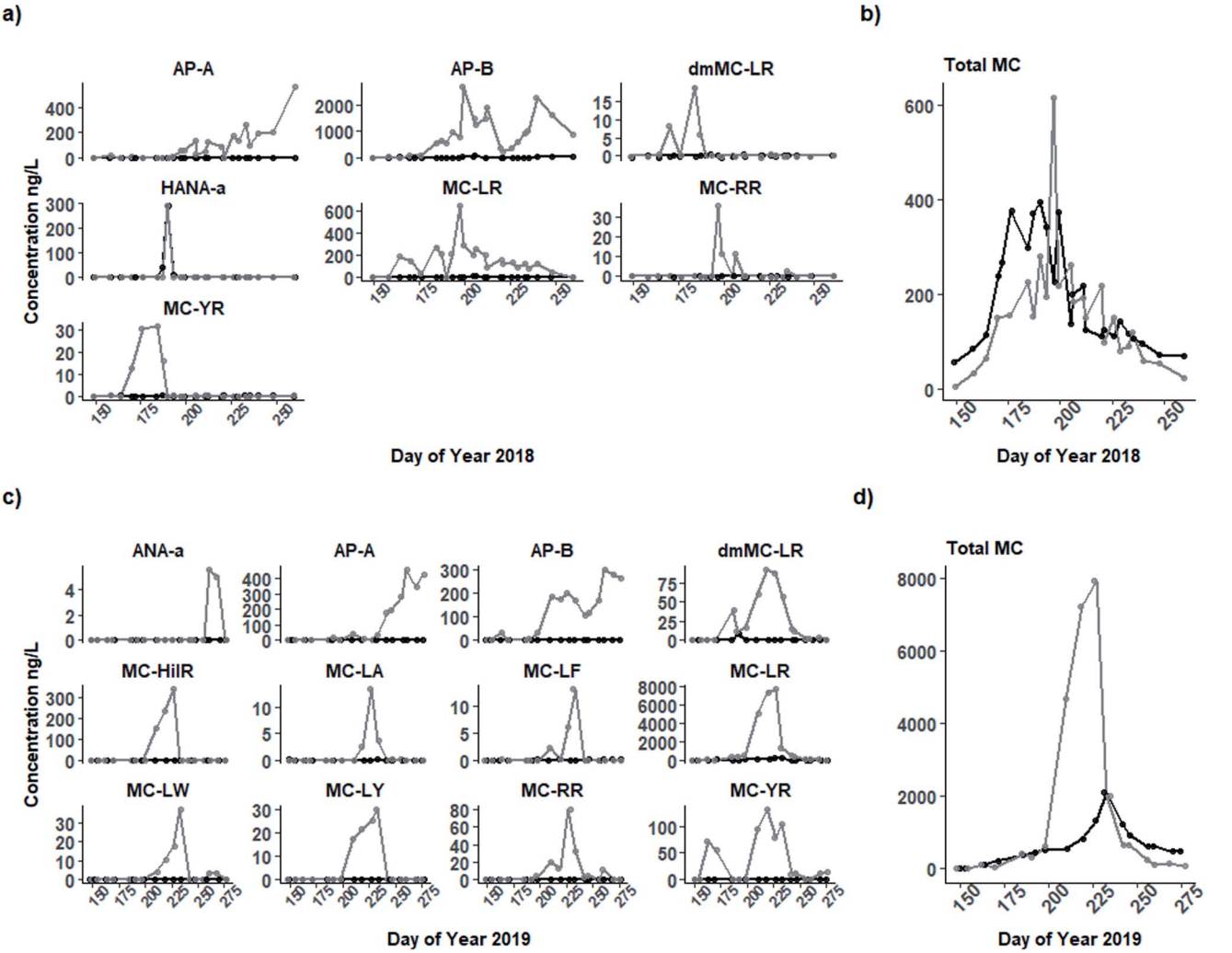

Fig. 4 Concentrations (ng L^{-1}) of screened intracellular (grey line) and extracellular (black line) cyanobacterial metabolites present in water from the 0.8 m depth of Buffalo Pound Lake in 2018 (a) and 2019 (c) including individual metabolites and total microcystins ("Total MC"; b, d). Only those metabolites that were present above the limit of detection (see Table S1†) in each year are shown.

concentrations occurring at the end of the sampling period coinciding with Group C.

Total microcystins. The most notable difference in concentrations between years was that of total microcystins. Concentrations of total microcystins were greatest in intracellular samples from Buffalo Pound Lake in both 2018 and 2019; however, concentrations in 2019 were more than an order of magnitude greater (Fig. 4b and d). Total microcystin concentrations in 2018 ranged from <1.0 to 616 ng L^{-1} in intracellular samples and 376 ng L^{-1} in extracellular samples. In 2019, intracellular total microcystins ranged from < 10 ng L^{-1} in late May and early June to nearly 8000 ng L^{-1} in mid-August. Extracellular total microcystins were lower, albeit still much greater than 2018 levels, ranging from <5.0 to more than 2000 ng L^{-1} (on DOY 227) during the same period. These maximum microcystin concentrations are well below the World Health Organization recreational exposure guideline (24 μg L^{-1}) and the guideline for short-term exposure (12 μg L^{-1}).[51] Because total microcystins in extracellular samples were orders of magnitude higher than any individual microcystin congener (see black lines in Fig. 4), it is likely there are unknown microcystins or their transformation products present in Buffalo Pound in addition to the screened common metabolites.

Individual cyanometabolites. Analysis of individual cyanobacterial metabolites revealed seven individual metabolites present above LOQ in 2018 and 12 individual metabolites present at concentrations above LOQ in 2019 in intracellular samples (Fig. 4a). In 2018, only homo-anatoxin was present in extracellular samples (from DOY 184 to 193, Group A) in addition to total microcystins, reaching a peak concentration of 288 ng L^{-1} on DOY 190 in early July. Intracellular toxins present in 2018 included anabaenopeptins A and B, four microcystin congeners (MC-LR, dmMC-LR, MC-RR, and MC-YR), and homo-anatoxin. Microcystins occurred predominately as the congener MC-LR and peaked by mid-July on DOY 197 before falling sharply by half (MC-LR = 293 ng L^{-1} on DOY 199). Anabaenopeptin B concentrations increased gradually from ~100 ng L^{-1}

in late June to ~1000 ng L^{-1} in mid-July on DOY 197, and then more than doubled between DOY 197 and 199, reaching 2706 ng L^{-1} on DOY 199 immediately following the drop in microcystin concentration. Anabaenopeptin B fell to 228 ng L^{-1} by mid-August (DOY 221) but peaked a second time (2296 ng L^{-1}) on DOY 240. Anabaenopeptin A also began to increase after microcystins declined with the highest concentration (570 ng L^{-1}) observed on the last day of sampling in September (DOY 260).

Of the 12 individual metabolites present in 2019 intracellular samples, nine were microcystin congeners (MC-LR, dmMC-LR, MC-HiIR, MC-LA, MC-LF, MC-LW, MC-LY, MC-RR, and MC-YR), and the remainder included anabaenopeptin A and B, and anatoxin-A (Fig. 4c). Only MC-LR and dmMC-LR were present in extracellular samples, both below 50 ng L^{-1}. As in 2018, the most prevalent microcystin congener in intracellular samples was MC-LR (from <10 to 7664 ng L^{-1}); MC-LR and the other microcystin congeners present peaked in mid-August (DOY 227), approximately one month later than in 2018 but again corresponding with Group B. Anatoxin-A was present in very small concentrations (below its LOQ, max = 6 ng L^{-1}) in September. Both anabaenopeptin A and B (max = 459 and 303 ng L^{-1}, respectively) peaked in September on DOY 260. Like in 2018, anabaenopeptin B concentrations also appeared to peak twice, the first smaller peak (202 ng L^{-1}) co-occurring with the microcystin peak and the second (303 ng L^{-1}) occurring on DOY 260. However, anabaenopeptin B was present at far lower concentrations in 2019 than in the previous year.

Co-occurrence of cyanotoxins and cyanobacterial species. The changing concentration and composition of intracellular cyanotoxins throughout the 2018 and 2019 sampling seasons co-occurred with changing cyanobacterial phytoplankton community composition as indicated by non-metric multidimensional scaling (NMDS) ordinations (2018 stress = 0.091;

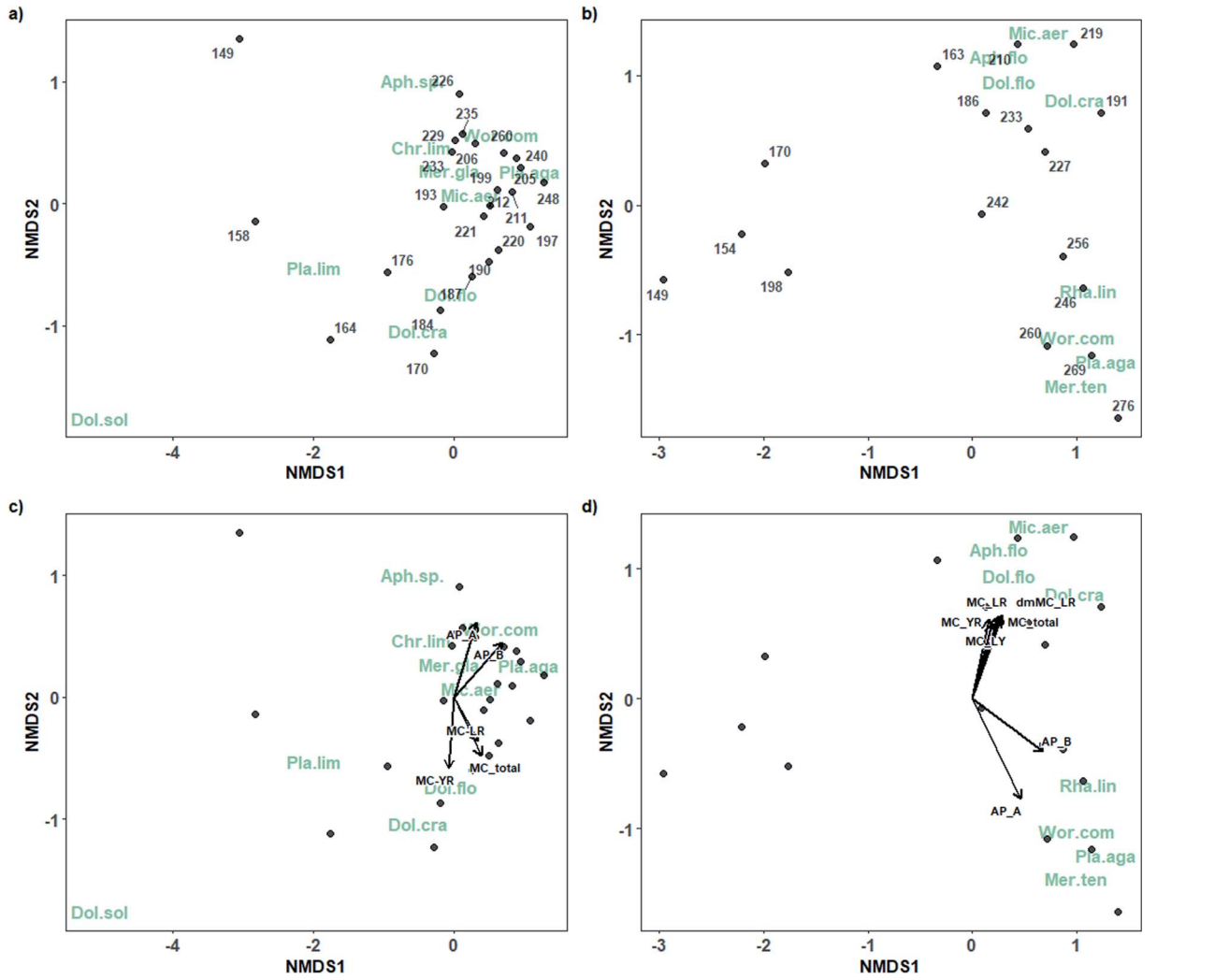

Fig. 5 Non-metric multidimensional scaling plots of cyanobacterial phytoplankton community composition throughout the 2018 (stress = 0.091; a, c) and 2019 (stress = 0.072; b, d) sampling seasons. Points indicate day of year in 2018 (a, c) and 2019 (b, d). Abbreviated species name codes using the first three letters of genus and species (gen.spe; shown in green) represent cyanobacterial species. Vectors represent toxins (see Table S1† for abbreviations) for which permutation tests were significant ($p > 0.05$) in 2018 (c) and 2019 (d) with vector length indicating strength of correlation.

2019 stress = 0.072; Fig. 5). Vectors, representing intracellular toxins and total microcystins, fit on to the ordinations point to distinct groups of species associated with microcystins and anabaenopeptins. Moreover, the composition of these groups was similar between years.

For example, in 2018, significant vectors showed an association between total microcystins ($r^2 = 0.39$, $p = 0.005$) and several microcystin congeners (dmMC-LR, $r^2 = 0.30$, $p = 0.035$; and MC-YR, $r^2 = 0.35$, $p = 0.016$) and the Group B (DOYs 184 to 212) cyanobacterial community dominated by diazotrophic taxa (*e.g.*, *D. crassa* and *D. flos-aquae*). The strongest associations were those between anabaenopeptin A ($r^2 = 0.48$, $p = 0.002$) and anabaenopeptin B ($r^2 = 0.68$, $p = 0.001$) and the late-season Group C (*e.g.*, DOYs 235 to 260) cyanobacterial community dominated by *Planktothrix agardhii*.

Similarly, in 2019, microcystins were also correlated with the mid-season (DOYs 186 to 227, or Group B) bloom comprised largely of the N-fixing taxa (*Dolichospermum flos-aquae*, *D. crassa*, *A. flos-aquae*) and which also included *Microcystis aeruginosa*. Total microcystins ($r^2 = 0.45$, $p = 0.014$) and four microcystin congeners, MC-LR ($r^2 = 0.47$, $p = 0.01$), dmMC-LR ($r^2 = 0.49$, $p = 0.008$), MC-LY ($r^2 = 0.37$, $p = 0.039$), and MC-YR ($r^2 = 0.39$, $p = 0.036$) were significantly correlated to the mid-season bloom cyanobacterial community. Anabaenopeptins A ($r^2 = 0.81$, $p = 0.001$) and B ($r^2 = 0.63$, $p = 0.001$) were most strongly correlated with the cyanobacterial community present after DOY 246 (Group C) which was largely dominated by *P. agardhii*, but also included *Woronichinia compacta*, *Rhabdogloea linearis*, and *Merismopedia tenuissima*.

Spearman rank correlations between the biomass of individual cyanobacterial species and the most prevalent intracellular cyanotoxins (total microcystins, anabaenopeptins A and B) in 2018 and 2019 were again suggestive of links between the Group B species and microcystins, and non-diazotrophic Group C species and anabaenopeptins. In 2018, correlations were strongest between total microcystins and diazotrophic *D. crassa* ($r_s = 0.68$, $p < 0.001$) as well as *D. flos-aquae* ($r_s = 0.57$, $p = 0.003$) and non-diazotrophic *M. aeruginosa* ($r_s = 0.52$, $p = 0.009$). Anabaenopeptin A was most strongly correlated with *W. compacta* biomass ($r_s = 0.78$, $p < 0.001$) and *P. agardhii* ($r_s = 0.49$, $p = 0.01$) but also negatively correlated with *D. crassa* ($r_s = -0.53$, $p = 0.007$) and *D. flos-aquae* ($r_s = -0.49$, $p = 0.02$). Anabaenopeptin B was most strongly correlated with *P. agardhii* ($r_s = 0.76$, $p < 0.001$) and *W. compacta* ($r_s = 0.57$, $p = 0.003$).

Of the Spearman rank correlations between the biomass of cyanobacterial species present in 2019 and intracellular toxins, the strongest was between total microcystins and *A. flos-aquae* ($r_s = 0.92$, $p < 0.001$). Significant positive correlations also existed between total microcystins and *D. crassa* ($r_s = 0.74$, $p = 0.001$), *D. flos-aquae* ($r_s = 0.72$, $p = 0.001$), *M. aeruginosa* ($r_s = 0.69$, $p = 0.002$), and *R. lineare* ($r_s = 0.56$, $p = 0.02$). Anabaenopeptin A was most strongly correlated with *P. agardhii* ($r_s = 0.77$, $p < 0.001$) and *W. compacta* biomass ($r_s = 0.78$, $p < 0.001$) as well as *M. tenuissima* ($r_s = 0.67$, $p = 0.002$). Anabaenopeptin B was correlated with the same species (*P. agardhii*, $r_s = 0.65$, $p = 0.004$; *W. compacta*, $r_s = 0.64$, $p = 0.006$; *M. tenuissima*, $r_s = 0.61$, $p = 0.008$) although these correlations were slightly weaker; however, it should be stated that correlations between individual species biomass and cyanopeptides are not indicative of a causal relationship between a particular species and the production of a cyanopeptide.

When the results of the Spearman rank correlations are taken into consideration alongside the results of the indicator species analysis, some key similarities are apparent. For example, *D. crassa* was an indicator for Group B in 2018, and the combination Group B + C in 2019, and *A. flos-aquae* was an indicator of Group B in 2018. Both species were strongly correlated with microcystins suggesting that they serve as important indicators of potentially toxic mid-summer bloom formation. *W. compacta* was an indicator of Group C in both years and correlated with the anabaenopeptins. Its presence appears to indicate a shift from a primarily microcystin-producing N-fixing bloom to an anabaenopeptin-producing bloom comprised largely of filamentous *Planktothrix*.

Comparison of taxonomy and chlorophyll-*a*

The period when *Planktothrix* dominated the community leading to high biomass was not accompanied by a similar peak in chl-*a*, suggesting it is not well indicated by chl-*a* (Fig. 6). In both years, when *Planktothrix agardhii* biomass was greatest in September (Fig. 6a), chl-*a* concentrations measured from the same parcel of water from which taxonomy samples were collected were relatively low (Fig. 6b). For example, in 2018, the highest chl-*a* concentration (92 μg L^{-1}) occurred in early July (DOY 190), while peak Planktothrix biomass (>10 000 mg m^{-3}) and near peak total biomass (>12 500 mg m^{-3}) occurred in early September (DOY 248) when chl-*a* was only 20 μg L^{-1}. Similarly, in 2019 chl-*a* reached peak concentration (118 μg L^{-1}) in early August (DOY 219) but had dropped to 29 μg L^{-1} when *Planktothrix* (>18 500 mg m^{-3}) and total biomass (>21 000 mg m^{-3}) were at their peak on DOY 260 in mid-September. Spearman rank correlations between *Dolichospermum* biomass and chl-*a* were significant ($p < 0.001$, $r_s = 0.66$ and $p < 0.001$, $r_s = 0.80$ in 2018 and 2019, respectively) while those between and *Planktothrix* biomass and chl-*a* were not significant in either year ($p = 0.09$, $r_s = 0.35$ and $p = 0.57$, $r_s = 0.15$ in 2018 and 2019, respectively; Fig. S2†).

Discussion

Cyanobacterial blooms in drinking water sources, such as Buffalo Pound Lake, can increase risks to water treatment operations. Consequently, managers are required to carefully monitor bloom-impacted systems with tools such as chl-*a* that can provide rapid information to ensure treatment processes remain unaffected by cyanobacteria. Here we have demonstrated the progression of cyanobacteria-dominated blooms from *Dolichospermum*-dominated diazotrophs to *Planktothrix agardhii* (a species that appears to evade detection by chl-*a*) in a critical drinking water supply and have identified the potential for each bloom phase to produce different suites of cyanotoxins. Moreover, we discerned that key indicator phytoplankton species can be valuable monitoring tools to help anticipate the

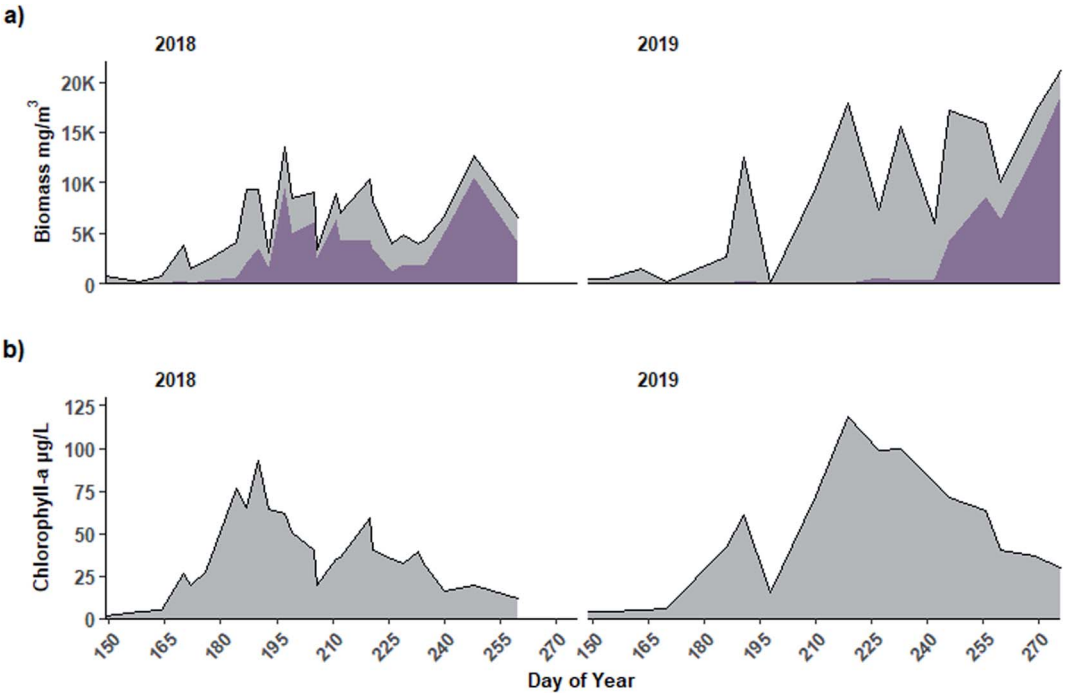

Fig. 6 (a) Total phytoplankton biomass (grey shaded area) including *Planktothrix agardhii* biomass (darker purple shading) and (b) chlorophyll-*a* concentration measured in samples collected from 0.8 m depth in Buffalo Pound Lake, Saskatchewan in 2018 and 2019.

timing, magnitude, and toxin dynamics of cyanobacterial bloom phases.

Our results showed that phytoplankton community structure near the Buffalo Pound Water Treatment Plant's raw water intake changed seasonally but did so in a consistent pattern during the two study years. Cryptophytes and chrysophytes (*i.e.*, Group A) were succeeded by N-fixing cyanobacteria, especially *Dolichospermum* spp. (*i.e.*, Group B). By September much of the community was composed of non-diazotrophic *Planktothrix agardhii* (*i.e.*, Group C). Though this general pattern was consistent between years, the timing of succession between groups differed as did their abundance. This succession from non-cyanobacterial species to a diazotroph-dominated community in the warm summer months is well established for many temperate eutrophic lakes.[52,53] In the prairie region, diazotrophic blooms have received much research attention by limnologists[11,54,55] given highly productive prairie systems tend towards N-limitation, a demonstrated driver of diazotrophic abundance.[56] The secondary late-season *Planktothrix* bloom exhibited in our study has received comparatively little research in prairie systems. We noted active N-fixation verified by the presence of heterocytes during the diazotrophic bloom phase but the mechanism leading to diazotrophic collapse and replacement with *Planktothrix* remains unclear given low inorganic N (*e.g.*, median September ammonium = ~30 µg N/L and nitrate = <LOD; Fig. S3†) typically persists late into the ice-free season.

Accompanying the above pattern of species succession was a shift in the cyanometabolites identified at our study site from microcystins in mid-summer to anabaenopeptins in early autumn. Cyanometabolites are detected frequently when cyanobacterial species are present and many species, including those identified here, can produce commonly detected compounds including microcystins and anabaenopeptins – the production of which may co-occur with each other or other cyanometabolites.[2,57] For example, the *Microcystis*, *Dolichospermum*, and *Planktothrix* species we identified are known producers of microcystins[58] and *Microcystis* and *Planktothrix* are also commonly shown to produce anabaenopeptins.[57,59] However, organisms that appear morphologically the same may in fact possess unique biosynthetic gene clusters differentiating their toxin-producing abilities;[60,61] therefore, causal attribution of cyanotoxin production to any one species is beyond the scope of the work presented here, requiring metatranscriptomics to verify activation of genes responsible for cyanopeptide synthesis.[60,62] Instead, we have identified patterns of co-occurrence with indicator species to establish the utility of such indicators for enhanced biomonitoring of bloom-prone systems.

The observed production of microcystins during the mid-season bloom was expected. Increased probabilities of microcystin concentrations exceeding public health thresholds in mid-summer have been described in Buffalo Pound and other prairie lakes previously.[12] Indeed, well-known microcystin producers (*D. crassa*, *D. flos-aquae*, *M. aeruginosa*, and in 2018 *P. agardhii*) occurred in Buffalo Pound in mid-summer, one of which, *Dolichospermum crassa*, served well as a specific indicator of that bloom phase in both years. Notably, during the mid-summer bloom period, total microcystins in extracellular samples were often higher than the sum of the 12 common

individual congeners targeted by our methods – a finding suggestive of the presence of unknown microcystins, of which there are more than 200 known microcystin congeners.[63] Another possibility is that transformation products were present containing the ADDA moiety detected by our total microcystin analysis. Such transformation products may contribute to potential toxicity of drinking/recreational waters,[58] thus their inclusion with the total microcystin concentrations reported here is warranted to assess risk.

The shift to an anabaenopeptin-producing community in early autumn dominated by *Planktothrix agardhii* was suggestive of either (1) a change in the metabolite producing species, or (2) some shift in metabolite production owing to environmental factors; however, confirmation of this finding with genomic tools is needed. Detection and subsequent study of anabaenopeptins in surface waters is relatively new;[64] however, many of the species we identified in our study, including the abundant *Planktothrix agardhii*[59] and our Group C indicator, *Woronichinia compacta*,[65] may produce anabaenopeptins. In both years, the detected concentrations of intracellular anabaenopeptins in Buffalo Pound increased as *Planktothrix* biomass increased. Moreover, anti-correlation was observed between *Dolichospermum* species (*D. crassa* and *D. flos-aquae*) biomass and anabaenopeptin A in 2018 while no correlations were observed between *Dolichospermum* biomass and anabaenopeptins A or B otherwise. While the pathway leading to this observation is unresolved and definitive attribution of anabaenopeptin production to *Planktothrix* or any other species is beyond the scope of the work presented here, our observation of a large *Planktothrix* bloom, indicated by *W. compacta* and accompanied by the presence of anabaenopeptins late in the year is notable given this secondary bloom has been relatively understudied and potential risks associated with anabaenopeptins remain unclear.[64]

Environmental conditions are likely to play a role in bloom succession from diazotrophs to *Planktothrix* and should be another focus of future research examining the understudied autumn bloom. *Planktothrix agardhii* has been shown to thrive and form large blooms under very low to non-detectable inorganic N concentrations[66] therefore a shift in nutrient availability is unlikely to explain why *Planktothrix* formed blooms under low inorganic N conditions in autumn (Fig. S3†). It is more likely the proliferation of *Planktothrix* is related to its tolerance of seasonal cooling and decreased solar irradiance.[59] Day length measured at the nearest weather station (Environment and Climate Change Canada station at Moose Jaw, SK) decreases from 16.35 hours on July 1 (∼DOY 182) to 11.63 hours on October 1 (∼DOY 270).[67] The late-season water temperatures in Buffalo Pound of just above 16 °C in early September (DOY ∼245) to 5–8 °C in early October (DOY ∼270, Fig. S4†) are well below the ideal range for *Dolichospermum* spp.[68] but still tolerable for *Planktothrix agardhii* which has been shown to persist as the dominant species even under ice.[69] For example, a similar study of a temperate lagoon by Pilkaitytė *et al.*[70] has shown dominance of N-fixing species (*A. flos-aquae* and *Dolichospermum* spp.) during the hot summer months while *Planktothrix agardhii* and *Woronichinia* spp. co-occurred in the cool autumn season, often achieving their highest biomass at that time – a finding consistent with the work presented here.

In addition to tolerating low temperatures, *Planktothrix* spp. are capable of photoheterotrophy and can energize slow filament growth using in-lake carbon sources even at very low irradiance.[71] Notably, cyanometabolites, such as microcystins and anabaenopeptins, are rich in C and N and may serve as major nutrient sources to heterotrophic bacteria that occur concurrently with phytoplankton blooms.[72,73] These nutrient-rich peptides, as well as other complex molecules produced by cyanobacteria, are taken up and subsequently re-mineralized by heterotrophs – a pathway that could serve as an important labile nutrient source to *Planktothrix* during photoheterotrophy.[72,74] *Planktothrix* may also use these cyanopeptides as a defense mechanism in response to microbial antagonists as illustrated by Rohrlack *et al.*[75] or to displace other bloom-forming cyanobacterial species *via* niche construction.[59,72,76] However, these compounds were largely detected in intracellular samples (*e.g.*, anabaenopeptins) thus their purpose, and the species responsible for their production, is unclear. It is also possible that rapid breakdown or uptake by heterotrophs in surface waters limits extracellular detection of these compounds.

We found that chl-*a* concentrations correlated well with *Dolichospermum* but did not capture the later *Planktothrix* bloom, suggesting reliance on photosynthesis is diminished later in the ice-free season. This finding may support the hypothesis that *Planktothrix* in Buffalo Pound are photoheterotrophic because less light is required to energize photoheterotrophy than photosynthesis;[71,77] thus, likely resulting in reduced chl-*a* production late in the season when irradiance is low. However, it is also possible that commonly used methods to measure chl-*a* may not always detect *Planktothrix* spp. biomass. For example, Wentzky *et al.*[78] reported this lack of association for *P. rubescens* due to the red pigment phycoerythrin which is detected at different wavelengths (*e.g.*, 525 and 570 nm (ref. 79)) than those commonly used to detect chl-*a* (*e.g.*, 659, 655, and 750 nm; see methods). *Planktothrix* in Buffalo Pound was identified as *P. agardhii*, or "green" *Planktothrix*, which typically lacks phycoerythrin.[80] However, morphology alone may not be sufficient to identify similar species within the same genera.[81] Recent work has shown *P. agardhii* and *P. rubescens* can have significant genetic overlap, including horizontal gene transfer of the phycoerythrin gene cluster between the two species thus resulting in both red and green phenotypes.[82,83] It is conceivable that *P. rubescens* existed in Buffalo Pound or, more likely, its deeper upstream reservoir previously, therefore an extremely low light adapted "red" phenotype of *P. agardhii* is a possibility; however algal filaments with red coloration have not been noted in raw intake water at the water treatment plant (Blair Kardash, BPWTP, pers. comm.).

Our results indicate that, under current conditions, the *Planktothrix* bloom associated with anabaenopeptins poses a potential but unknown risk to human and wildlife health.[84] *Planktothrix* was not correlated with toxic microcystins like the earlier *Dolichospermum* bloom. However, anabaenopeptin toxicity is less studied than microcystin toxicity.[72] Yet despite the correlations we have found, without deeper analysis (*e.g.*, at

the metatranscriptomic level) we cannot conclude that a particular species has a causal relationship with any individual cyanobacterial metabolite. Besides, toxicogenic strains of *P. agardhii* have been widely observed elsewhere in temperate Canadian systems (*e.g.*, in Lake Erie[85]) and environmental drivers may in fact mediate toxin-producing gene activity;[59,62] thus, it is possible that toxin expression by the late season *Planktothrix* bloom in Buffalo Pound may change depending on other factors not explored here (*e.g.*, changing climatic conditions or nutrient sources). As such, continued monitoring and study of this important late season bloom is needed to establish possible toxin risk.

The largest amount of biomass during the sampling period in both years was recorded during the *Planktothrix* bloom. Given that *Planktothrix* is both filamentous and can potentially produce toxins, the ability to detect it is critical for drinking water operations. However, our results show that the most cost-effective and easy-to-use chl-*a* sensors and laboratory methods may not provide operators with reliable indication of increasing *Planktothrix* biomass as solar irradiance declines later in the year. We found the presence of *Woronichinia compacta* to be a good indicator of the conditions in which large *Planktothrix* blooms occurred, but, given the abundance of *Planktothrix* compared to *W. compacta*, drinking water operators who routinely use microscopy are likely to find *Planktothrix* itself easier to target and identify in their weekly samples. Such information can be used to supplement chl-*a* concentrations and algal cell counts to allow for better preparation for potential water treatment challenges posed by large amounts of buoyant, filamentous biomass. However, identification of indicators may require technicians to go beyond the basic algal identification outlined in standard methods. Given the scale and urgency of the problems posed by cyanobacterial blooms, updated guidance for the identification of cyanobacterial species should therefore be a priority for regulators.

Our finding of common seasonal patterns and indicators each year suggests there may be underlying stability to community structure albeit the time period presented here is limited thus additional years of study would be needed to make such conclusions. We hypothesize that environmental variables are likely driving the differences in magnitude and timing of blooms and their associated cyanotoxins observed in the two years. For example, succession between community groups occurred earlier in 2018 than in 2019 and the cyanobacterial community was, for the most part, *Planktothrix*-dominated after mid-July. However, in 2019, the bloom phases occurred two weeks to one month later, with the *Planktothrix* bloom only taking hold at the end of August. Moreover, N-fixation and diazotrophic abundance was also greater in 2019. These findings point to differences in nutrient availability and climatic conditions (*e.g.*, temperature, precipitation, wind, and runoff) potentially acting to modulate bloom formation and collapse. Future work should explore the environmental drivers of the bloom phylogeny illustrated here to better enable the prediction of these distinct bloom phases.

Conclusion

Our work has shown two distinct cyanobacterial bloom phases in the ice-free months, one dominated by diazotrophs and the presence of microcystins, the other by abundant *Planktothrix* biomass and the presence of anabaenopeptins. Each present unique challenges to water treatment operators; however, biomass indicators (*e.g.*, chl-*a*) and microscopically identified indicator species can be used together by managers to aid in the prediction and mitigation of bloom impacts on drinking water production. Genetic analysis of the autumn cyanobacterial community could help reconcile the taxonomic identification of *Planktothrix agardhii* in Buffalo Pound Lake with possible morphological plasticity;[61] however, effective management relies on methods that yield rapid results and are within-reach of water treatment managers. We also caution that although chl-*a* remains an important tool given its correlation with the microcystin-producing mid-season bloom here, it may not be ideal for assessing localized bloom risk in autumn when *Planktothrix* is a dominant bloom-forming species. For example, BPWTP attempted cessation of autumn pre-chlorination in 2021, and, despite low sensor-detected chl-*a* in the lake, found buoyant floc accumulating in the clarifiers within 12 hours co-occurring with positive identification of *Planktothrix via* in-house microscopy of raw intake water (Blair Kardash, BPWTP, pers. comm.).

The similarity in patterns observed over two years is certainly useful to understand this complex system but it is not certain that those two years are representative of current or future conditions in Buffalo Pound Lake. With mounting threats to water security in the Saskatchewan River Basin,[34] and large-scale irrigation development planned[86] directly upstream, understanding and protection of this key drinking water resource in the face of change is increasingly critical. Climate models for the prairie region continue to point to increased future warming[87] and there is a growing body of evidence suggesting harmful blooms and their toxins will increase in shallow, polymictic prairie lakes like Buffalo Pound.[12] The impacts of this warming may be an increasingly toxic mid-season N-fixing bloom which could exacerbate the challenges for toxin removal. The potential for increased landscape runoff from more severe precipitation events could bring further water treatment challenges related to disinfection by-products if delivery of DOM to the lake increases. Autumn irradiance will remain low regardless, thus with longer ice-free seasons induced by climate warming, filamentous *Planktothrix* is likely to proliferate in deeper areas of the lake (*e.g.*, near BPWTP intake) later into the year—as suggested by recent reports of *P. agardhii* blooms (and toxins) persisting through the winter under ice.[69] Improved understanding of the autumn *Planktothrix* bloom, its persistence, and its potential to produce toxins will be increasingly important, thus we recommend targeted study of this key bloom phase, and its potential indicators, in the future.

Open research statement

The taxonomy, cyanotoxin, and nutrient data, figures and associated code used to describe the cyanobacterial community

of Buffalo Pound Lake are available at https://doi.org/10.5683/SP3/MP6NXF.

Conflicts of interest

There are no conflicts to declare.

Acknowledgements

Research funding for this work was generously provided by the Canada First Research Excellence Fund as part of the Global Water Futures Initiative FORMBLOOM (Forecasting Tools and Mitigation Options for Diverse Bloom-Affected Lakes) in addition to ATRAPP (Algal Blooms, Treatment, Risk Assessment, Prediction and Prevention through Genomics) from Genome Canada and Genome Québec. Funding was also provided through an academic-industry partnership with the Buffalo Pound Water Treatment Plant supported by the Mitacs Accelerate program. We wish to sincerely thank Blair Kardash, Laboratory and Research Manager at the Buffalo Pound Water Treatment Plant for guidance, advice, cooperation and thoughtful insight about the lake and treatment processes. We also wish to thank Katy Nugent and members of the SaskWatChE Lab for sample collection and nutrient analyses, Quoc Tuc Dinh for cyanotoxin analysis, Lisa Boyer for data/code assistance, and Colin Whitfield and Luis Morales-Marin for shapefiles of the drainage areas surrounding Buffalo Pound Lake. Lastly, we thank the two anonymous reviewers who provided thoughtful insight and improved the quality of our paper.

References

1 J. C. Ho, A. M. Michalak and N. Pahlevan, Widespread global increase in intense lake phytoplankton blooms since the 1980s, *Nature*, 2019, **574**, 667–670, DOI: 10.1038/s41586-019-1648-7.

2 J. Huisman, G. A. Codd, H. W. Paerl, B. W. Ibelings, J. M. Verspagen and P. M. Visser, Cyanobacterial blooms, *Nat. Rev. Microbiol.*, 2018, **16**, 471–483, DOI: 10.1038/s41579-018-0040-1.

3 Z. E. Taranu, I. Gregory-Eaves, P. R. Leavitt, L. Bunting, T. Buchaca, J. Catalan, I. Domaizon, P. Guilizzoni, A. Lami, S. McGowan, H. Moorhouse, G. Morabito, F. R. Pick, M. A. Stevenson, P. L. Thompson and R. D. Vinebrooke, Acceleration of cyanobacterial dominance in north temperate-subarctic lakes during the Anthropocene, *Ecol. Lett.*, 2015, **18**, 375–384, DOI: 10.1111/ele.12420.

4 J. Heisler, P. M. Glibert, J. M. Burkholder, D. M. Anderson, W. Cochlan, W. C. Dennison, Q. Dortch, C. J. Gobler, C. A. Heil, E. Humphries, A. Lewitus, R. Magnien, H. G. Marshall, K. Sellner, D. A. Stockwell, D. K. Stoecker and M. Suddleson, Eutrophication and harmful algal blooms: a scientific consensus, *Harmful Algae*, 2008, **8**, 3–13, DOI: 10.1016/j.hal.2008.08.006.

5 S. Kosten, V. L. Huszar, E. Bécares, L. S. Costa, E. van Donk, L. A. Hansson, E. Jeppesen, C. Kruk, G. Lacerot, N. Mazzeo, L. De Meester, B. Moss, M. Lürling, T. Nõges, S. Romo and M. Scheffer, Warmer climates boost cyanobacterial dominance in shallow lakes, *Global Change Biol.*, 2012, **18**, 118–126, DOI: 10.1111/j.1365-2486.2011.02488.x.

6 H. W. Paerl and J. Huisman, Climate change: a catalyst for global expansion of harmful cyanobacterial blooms, *Environ. Microbiol. Rep.*, 2009, **1**, 27–37, DOI: 10.1111/j.1758-2229.2008.00004.x.

7 D. M. Orihel, D. F. Bird, M. Brylinsky, H. Chen, D. B. Donald, D. Y. Huang, A. Giani, D. Kinniburgh, H. Kling, B. G. Kotak, P. R. Leavitt, C. C. Nielsen, S. Reedyk, R. C. Rooney, S. B. Watson, R. W. Zurawell and R. D. Vinebrooke, High microcystin concentrations occur only at low nitrogen-to-phosphorus ratios in nutrient-rich Canadian lakes, *Can. J. Fish. Aquat. Sci.*, 2012, **69**, 1457–1462, DOI: 10.1139/f2012-088.

8 D. W. Schindler and W. F. Donahue, An impending water crisis in Canada's western prairie provinces, *Proc. Natl. Acad. Sci.*, 2006, **103**, 7210–7216, DOI: 10.1073/pnas.0601568103.

9 C. E. Binding, T. A. Greenberg, G. McCullough, S. B. Watson and E. Page, An analysis of satellite-derived chlorophyll and algal bloom indices on Lake Winnipeg, *J. Great Lake. Res.*, 2018, **44**, 436–446, DOI: 10.1016/j.jglr.2018.04.001.

10 G. Ali and C. English, Phytoplankton blooms in Lake Winnipeg linked to selective water-gatekeeper connectivity, *Sci. Rep.*, 2019, **9**, 1–10, DOI: 10.1038/s41598-019-44717-y.

11 L. Bunting, P. R. Leavitt, G. L. Simpson, B. Wissel, K. R. Laird, B. F. Cumming, A. St. Amand and D. R. Engstrom, Increased variability and sudden ecosystem state change in Lake Winnipeg, Canada, caused by 20th century agriculture, *Limnol. Oceanogr.*, 2016, **61**, 2090–2107, DOI: 10.1002/lno.10355.

12 N. M. Hayes, H. A. Haig, G. L. Simpson and P. R. Leavitt, Effects of lake warming on the seasonal risk of toxic cyanobacteria exposure, *Limnol. Oceanogr. Lett.*, 2020, **5**, 393–402, DOI: 10.1002/lol2.10164.

13 T. J. Tse, L. E. Doig, S. Tang, X. Zhang, W. Sun, S. B. Wiseman, C. Xin Feng, H. Liu, J. P Giesy, M. Hecker and P. D. Jones, Combining high-throughput sequencing of *sedaDNA* and traditional paleolimnological techniques to infer historical trends in cyanobacterial communities, *Environ. Sci. Technol.*, 2018, **52**, 6842–6853, DOI: 10.1021/acs.est.7b06386.

14 C. J. Loewen, R. D. Vinebrooke and R. W. Zurawell, Quantifying seasonal succession of phytoplankton trait-environment associations in human-altered landscapes, *Limnol. Oceanogr.*, 2021, **66**, 1409–1423, DOI: 10.1002/lno.11694.

15 D. W. Schindler, R. E. Hecky and G. K. McCullough, The rapid eutrophication of Lake Winnipeg: Greening under global change, *J. Great Lake. Res.*, 2012, **38**, 6–13, DOI: 10.1073/pnas.0601568103.

16 J. J. Gibson, S. J. Birks, Y. Yi, M. C. Moncur and P. M. McEachern, Stable isotope mass balance of fifty lakes in central Alberta: Assessing the role of water balance parameters in determining trophic status and lake level, *J.*

Hydrol.: Reg. Stud., 2016, **6**, 13–25, DOI: **10.1016/j.ejrh.2016.01.034**.

17 P. M Visser, J. M. Verspagen, G. Sandrini, L. J. Stal, H. C. Matthijs, T. W. Davis, H. W. Paerl and J. Huisman, How rising CO_2 and global warming may stimulate harmful cyanobacterial blooms, *Harmful Algae*, 2016, **54**, 145–159, DOI: **10.1016/j.hal.2015.12.006**.

18 F. Jalili, H. Trigui, J. F. Guerra Maldonado, S. Dorner, A. Zamyadi, B. J. Shapiro, Y. Terrat, N. Fortin, S. Sauvé and M. Prévost, Can Cyanobacterial Diversity in the Source Predict the Diversity in Sludge and the Risk of Toxin Release in a Drinking Water Treatment Plant?, *Toxins*, 2021, **13**, 25, DOI: **10.3390/toxins13010025**.

19 A. Zamyadi, C. Romanis, T. Mills, B. Neilan, F. Choo, L. A. Coral, D. Gale, G. Newcombe, N. Crosbie, R. Stuetz and R. K. Henderson, Diagnosing water treatment critical control points for cyanobacterial removal: Exploring benefits of combined microscopy, next-generation sequencing, and cell integrity methods, *Water Res.*, 2019, **152**, 96–105, DOI: **10.1016/j.watres.2019.01.002**.

20 World Health Organization, *Managing cyanobacteria in drinking water supplies: information for regulators and water suppliers*, WHO/FWC/WSH/15.03, 2011.

21 A. Zamyadi, C. M. Glover, A. Yasir, R. Stuetz, G. Newcombe, N. D. Crosbie, T. Lin and R. Henderson, Toxic cyanobacteria in water supply systems: data analysis to map global challenges and demonstrate the benefits of multi-barrier treatment approaches, *H2Open Journal*, 2021, **4**, 47–62, DOI: **10.2166/h2oj.2021.067**.

22 Public Health Agency of Canada, *Guidelines for Canadian Drinking Water Quality: Guideline Technical Document – Trihalomethanes*, 2013.

23 S. Moradinejad, C. M. Glover, J. Mailly, T. Z. Seighalani, S. Peldszus, B. Barbeau, S. Dorner, M. Prévost and A. Zamyadi, Using advanced spectroscopy and organic matter characterization to evaluate the impact of oxidation on cyanobacteria, *Toxins*, 2019, **11**, 278, DOI: **10.3390/toxins11050278**.

24 R. J. Vogt, S. Sharma and P. R. Leavitt, Direct and interactive effects of climate, meteorology, river hydrology, and lake characteristics on water quality in productive lakes of the Canadian Prairies, *Can. J. Fish. Aquat. Sci.*, 2018, **75**, 47–59, DOI: **10.1139/cjfas-2016-0520**.

25 Buffalo Pound Water, *Board of Directors Annual Report*, 2020.

26 A. Zamyadi, F. Choo, G. Newcombe, R. Stuetz and R. K. Henderson, A review of monitoring technologies for real-time management of cyanobacteria: Recent advances and future direction, *Trends Anal. Chem.*, 2016, **85**, 83–96, DOI: **10.1016/j.trac.2016.06.023**.

27 Health Canada, *Guidelines for Canadian Drinking Water Quality: Guideline Technical Document – Cyanobacterial Toxins*, 2021.

28 S. Dumanski, J. W. Pomeroy and C. J. Westbrook, Hydrological regime changes in a Canadian Prairie basin, *Hydrol. Process.*, 2015, **29**, 3893–3904, DOI: **10.1002/hyp.10567**.

29 Water Security Agency, Buffalo Pound Lake, **https://www.wsask.ca/lakes-rivers/dams-reservoirs/major-dams-and-reservoirs/buffalo-pound-lake/**, accessed July 2021.

30 J. A. Terry, A. Sadeghian and K. E. Lindenschmidt, Modelling dissolved oxygen/sediment oxygen demand under ice in a shallow eutrophic prairie reservoir, *Water*, 2017, **9**, 131, DOI: **10.3390/w9020131**.

31 J. Terry, PhD thesis, University of Saskatchewan, 2020.

32 Natural Resources Canada, CanVec, **https://maps.canada.ca/czs/index-en.html**, accessed November 2021.

33 Esri Canada & Natural Earth Vector, *ArcGIS Online via ArcGIS Pro 10.6*, Environmental Systems Research Institute, Redlands, CA, 2020.

34 H. Wheater and P. Gober, Water security in the Canadian Prairies: science and management challenges, *Philos. Trans. R. Soc., A*, 2013, **371**, 20120409, DOI: **10.1098/rsta.2012.0409**.

35 E. Cavaliere and H. M. Baulch, Winter in two phases: Long-term study of a shallow reservoir in winter, *Limnol. Oceanogr.*, 2021, **66**, 1335–1352, DOI: **10.1002/lno.11687**.

36 CTV News, *Buffalo Pound Lake outflows increased as water issues linger*, 2015.

37 A. Roy-Lachapelle, S. V. Duy, G. Munoz, Q. T. Dinh, E. Bahl, D. F. Simon and S. Sauvé, Analysis of multiclass cyanotoxins (microcystins, anabaenopeptins, cylindrospermopsin and anatoxins) in lake waters using on-line SPE liquid chromatography high-resolution Orbitrap mass spectrometry, *Anal. Methods*, 2019, **11**, 5289–5300, DOI: **10.1039/C9AY01132C**.

38 Q. T. Dinh, G. Munoz, D. F. Simon, S. V. Duy, B. Husk and S. Sauvé, Stability issues of microcystins, anabaenopeptins, anatoxins, and cylindrospermopsin during short-term and long-term storage of surface water and drinking water samples, *Harmful Algae*, 2021, **101**, 101955, DOI: **10.1016/j.hal.2020.101955**.

39 P. B. Fayad, A. Roy-Lachapelle, S. V. Duy, M. Prévost and S. Sauvé, On-line solid-phase extraction coupled to liquid chromatography tandem mass spectrometry for the analysis of cyanotoxins in algal blooms, *Toxicon*, 2015, **108**, 167–175, DOI: **10.1016/j.toxicon.2015.10.010**.

40 G. Munoz, S. V. Duy, A. Roy-Lachapelle, B. Husk and S. Sauvé, Analysis of individual and total microcystins in surface water by on-line preconcentration and desalting coupled to liquid chromatography tandem mass spectrometry, *J. Chromatogr. A*, 2017, **1516**, 9–20, DOI: **10.1016/j.chroma.2017.07.096**.

41 M. L. Larsen, H. M. Baulch, S. L. Schiff, D. F. Simon, S. Sauvé and J. J. Venkiteswaran, Extreme rainfall drives early onset cyanobacterial bloom, *FACETS*, 2020, **5**, 899–920, DOI: **10.1139/facets-2020-0022**.

42 D. L. Findlay and H. J. Kling, *Protocols for measuring biodiversity: phytoplankton in freshwater*, Department of Fisheries and Oceans, Winnipeg, Canada, 2003.

43 R. A. Vollenweider, Scientific fundamentals of the eutrophication of lakes and flowing waters, with particular reference to nitrogen and phosphorus as factors in

eutrophication, *Technical Report DAS/CS1/68.27*, vol. 3, Paris, France, 1968.

44 J. F. G. M. Wintermans and A. S. De Mots, Spectrophotometric characteristics of chlorophylls a and b and their phenophytins in ethanol, *Biochim. Biophys. Acta*, 1965, **109**, 448–453, DOI: **10.1016/0926-6585(65)90170-6**.

45 R Core Team, *R: A language and environment for statistical computing*, R Foundation for Statistical Computing v. 4. 0. 5, Vienna, Austria, 2021.

46 P. Legendre and E. D. Gallagher, Ecologically meaningful transformations for ordination of species data, *Oecologia*, 2001, **129**, 271–280, DOI: **10.1007/s004420100716**.

47 M. De Cáceres, P. Legendre and M. Moretti, Improving indicator species analysis by combining groups of sites, *Oikos*, 2010, **119**, 1674–1684, DOI: **10.1111/j.1600-0706.2010.18334.x**.

48 M. De Cáceres, F. Jansen and N. Dell, *Package 'indicspecies': Relationships between species and groups of sites*, 2020, **https://cran.r-project.org/web/packages/indicspecies/indicspecies.pdf**.

49 M. Dufrêne and P. Legendre, Species assemblages and indicator species: the need for a flexible asymmetrical approach, *Ecol. Monogr.*, 1997, **67**, 345–366, DOI: **10.1890/0012-9615(1997)067[0345:SAAIST]2.0.CO;2**.

50 J. Oksanen, *Package 'vegan' v. 2.6-2*, 2022, **https://cran.r-project.org/web/packages/vegan/vegan.pdf**.

51 World Health Organization, *Cyanobacterial toxins: microcystins. Background document for development of WHO Guidelines for drinking-water quality and Guidelines for safe recreational water environments*, WHO/HEP/ECH/WSH/2020.6, 2020.

52 D. M. Orihel, D. W. Schindler, N. C. Ballard, M. D. Graham, D. W. O'Connell, L. R. Wilson and R. D. Vinebrooke, The "nutrient pump:" Iron-poor sediments fuel low nitrogen-to-phosphorus ratios and cyanobacterial blooms in polymictic lakes, *Limnol. Oceanogr.*, 2015, **60**, 856–871, DOI: **10.1002/lno.10076**.

53 A. D. Persaud, A. M. Paterson, P. J. Dillon, J. G. Winter, M. Palmer and K. M. Somers, Forecasting cyanobacteria dominance in Canadian temperate lakes, *J. Environ. Manage.*, 2015, **151**, 343–352, DOI: **10.1016/j.jenvman.2015.01.009**.

54 M. J. Bogard, R. J. Vogt, N. M. Hayes and P. R. Leavitt, Unabated nitrogen pollution favors growth of toxic Cyanobacteria over Chlorophytes in most hypereutrophic lakes, *Environ. Sci. Technol.*, 2020, **54**, 3219–3227, DOI: **10.1021/acs.est.9b06299**.

55 N. M. Hayes, A. Patoine, H. A. Haig, G. L. Simpson, V. J. Swarbrick, E. Wiik and P. R. Leavitt, Spatial and temporal variation in nitrogen fixation and its importance to phytoplankton in phosphorus-rich lakes, *Freshwater Biol.*, 2019, **64**, 269–283, DOI: **10.1111/fwb.13214**.

56 S. N. Higgins, M. J. Paterson, R. E. Hecky, D. W. Schindler, J. J. Venkiteswaran and D. L. Findlay, Biological nitrogen fixation prevents the response of a eutrophic lake to reduced loading of nitrogen: evidence from a 46-year whole-lake experiment, *Ecosystems*, 2018, **21**, 1088–1100, DOI: **10.1007/s10021-017-0204-2**.

57 E. M. L. Janssen, Cyanobacterial peptides beyond microcystins–A review on co-occurrence, toxicity, and challenges for risk assessment, *Water Res.*, 2019, **151**, 488–499, DOI: **10.1016/j.watres.2018.12.048**.

58 D. Dziga, A. Maksylewicz, M. Maroszek, A. Budzyńska, A. Napiorkowska-Krzebietke, M. Toporowska, M. Grabowska, A. Kozak, J. Rosińska and J. Meriluoto, The biodegradation of microcystins in temperate freshwater bodies with previous cyanobacterial history, *Ecotoxicol. Environ. Saf.*, 2017, **145**, 420–430, DOI: **10.1016/j.ecoenv.2017.07.046**.

59 R. Kurmayer, L. Deng and E. Entfellner, Role of toxic and bioactive secondary metabolites in colonization and bloom formation by filamentous cyanobacteria Planktothrix, *Harmful Algae*, 2016, **54**, 69–86, DOI: **10.1016/j.hal.2016.01.004**.

60 J. Österholm, R. V. Popin, D. P. Fewer and K. Sivonen, Phylogenomic analysis of secondary metabolism in the toxic cyanobacterial genera Anabaena, Dolichospermum and Aphanizomenon, *Toxins*, 2020, **12**, 248, DOI: **10.3390/toxins12040248**.

61 S. Moradinejad, H. Trigui, J. F. Guerra Maldonado, J. Shapiro, Y. Terrat, A. Zamyadi, S. Dorner and M. Prévost, Diversity Assessment of Toxic Cyanobacterial Blooms during Oxidation, *Toxins*, 2020, **12**, 728, DOI: **10.3390/toxins12110728**.

62 M. J. Harke, T. W. Davis, S. B. Watson and C. J. Gobler, Nutrient-controlled niche differentiation of western Lake Erie cyanobacterial populations revealed via metatranscriptomic surveys, *Environ. Sci. Technol.*, 2016, **50**, 604–615, DOI: **10.1021/acs.est.5b03931**.

63 *Handbook of cyanobacterial monitoring and cyanotoxin analysis*, ed. J. Meriluoto, L. Spoof and G. A. Codd, John Wiley & Sons, 2017.

64 M. Skafi, S. V. Duy, G. Munoz, Q. T. Dinh, D. F. Simon, P. Juneau and S. Sauvé, Occurrence of microcystins, anabaenopeptins and other cyanotoxins in fish from a freshwater wildlife reserve impacted by harmful cyanobacterial blooms, *Toxicon*, 2021, **194**, 44–52, DOI: **10.1016/j.toxicon.2021.02.004**.

65 K. Häggqvist, A. Toruńska-Sitarz, A. Błaszczyk, H. Mazur-Marzec and J. Meriluoto, Morphologic, phylogenetic and chemical characterization of a brackish colonial picocyanobacterium (Coelosphaeriaceae) with bioactive properties, *Toxins*, 2016, **8**, 108, DOI: **10.3390/toxins8040108**.

66 J. J. Hampel, M. J. McCarthy, M. Neudeck, G. S. Bullerjahn, R. M. L. McKay and S. E. Newell, Ammonium recycling supports toxic Planktothrix blooms in Sandusky Bay, Lake Erie: Evidence from stable isotope and metatranscriptome data, *Harmful Algae*, 2019, **81**, 42–52, DOI: **10.1016/j.hal.2018.11.011**.

67 National Research Council of Canada, *Sunrise/Sunset Calculator*, **https://nrc.canada.ca/en/research-development/products-services/software-applications/sun-calculator/**, accessed April 2022.

68 R. Li and M. Watanabe, Physiological properties of planktic species of Anabaena (Cyanobacteria) and their taxonomic value at species level, *Arch. Hydrobiol., Suppl.*, 2001, **103**, 31–45, DOI: **10.1127/algol_stud/103/2001/31**.

69 Ł. Wejnerowski, P. Rzymski, M. Kokociński and J. Meriluoto, The structure and toxicity of winter cyanobacterial bloom in a eutrophic lake of the temperate zone, *Ecotoxicology*, 2018, **27**, 752–760, DOI: **10.1007/s10646-018-1957-x**.

70 R. Pilkaitytė, D. Overlingė, Z. R. Gasiūnaitė and H. Mazur-Marzec, Spatial and temporal diversity of cyanometabolites in the eutrophic Curonian Lagoon (SE Baltic Sea), *Water*, 2021, **13**, 1760, DOI: **10.3390/w13131760**.

71 T. Zotina, O. Köster and F. Jüttner, Photoheterotrophy and light-dependent uptake of organic and organic nitrogenous compounds by *Planktothrix rubescens* under low irradiance, *Freshwater Biol.*, 2003, **48**, 1859–1872, DOI: **10.1046/j.1365-2427.2003.01134.x**.

72 P. R. Monteiro, S. C. do Amaral, A. S. Siqueira, L. P. Xavier and A. V. Santos, Anabaenopeptins: What We Know So Far, *Toxins*, 2021, **13**, 522, DOI: **10.3390/toxins13080522**.

73 J. R. Seymour, S. A. Amin, J. B. Raina and R. Stocker, Zooming in on the phycosphere: the ecological interface for phytoplankton–bacteria relationships, *Nat. Microbiol.*, 2017, **2**, 1–12, DOI: **10.1038/nmicrobiol.2017.65**.

74 M. Toporowska, H. Mazur-Marzec and B. Pawlik-Skowrońska, The effects of cyanobacterial bloom extracts on the biomass, Chl-a, MC and other oligopeptides contents in a natural *Planktothrix agardhii* population, *Int. J. Environ. Res. Public Health*, 2020, **17**, 2881, DOI: **10.3390/ijerph17082881**.

75 T. Rohrlack, G. Christiansen and R. Kurmayer, Putative antiparasite defensive system involving ribosomal and nonribosomal oligopeptides in cyanobacteria of the genus Planktothrix, *Appl. Environ. Microbiol.*, 2013, **79**, 2642–2647, DOI: **10.1128/AEM.03499-12**.

76 B. Sedmak, S. Carmeli, M. Pompe-Novak, M. Tušek-Žnidarič, O. Grach-Pogrebinsky, T. Eleršek, M. C. Žužek, A. Bubik and R. Frangež, Cyanobacterial cytoskeleton immunostaining: the detection of cyanobacterial cell lysis induced by planktopeptin BL1125, *J. Plankton Res.*, 2009, **31**, 1321–1330, DOI: **10.1093/plankt/fbp076**.

77 A. Vonshak, S. M. Cheung and F. Chen, Mixotrophic growth modifies the response of Spirulina (Arthrospira) platensis (Cyanobacteria) cells to light, *J. Phycol.*, 2000, **36**, 675–679, DOI: **10.1046/j.1529-8817.2000.99198.x**.

78 V. C. Wentzky, M. A. Frassl, K. Rinke and B. Boehrer, Metalimnetic oxygen minimum and the presence of *Planktothrix rubescens* in a low-nutrient drinking water reservoir, *Water Res.*, 2019, **148**, 208–218, DOI: **10.1016/j.watres.2018.10.047**.

79 C. Fournier, E. Riehle, D. R. Dietrich and D. Schleheck, Is Toxin-Producing Planktothrix sp. an Emerging Species in Lake Constance?, *Toxins*, 2021, **13**, 666, DOI: **10.3390/toxins13090666**.

80 S. Suda, M. M. Watanabe, S. Otsuka, A. Mahakahant, W. Yongmanitchai, N. Nopartnaraporn, Y. Liu and J. G. Day, Taxonomic revision of water-bloom-forming species of oscillatorioid cyanobacteria, *Int. J. Syst. Evol. Microbiol.*, 2002, **52**, 1577–1595, DOI: **10.1099/00207713-52-5-1577**.

81 O. M. Pérez-Carrascal, Y. Terrat, A. Giani, N. Fortin, C. W. Greer, N. Tromas and B. J. Shapiro, Coherence of Microcystis species revealed through population genomics, *ISME J.*, 2019, **13**, 2887–2900, DOI: **10.1038/s41396-019-0481-1**.

82 A. Tooming-Klunderud, H. Sogge, T. B. Rounge, A. J. Nederbragt, K. Lagesen, G. Glöckner, P. K. Hayes, T. Rohrlack and K. S. Jakobsen, From green to red: Horizontal gene transfer of the phycoerythrin gene cluster between Planktothrix strains, *Appl. Environ. Microbiol.*, 2013, **79**, 6803–6812, DOI: **10.1128/AEM.01455-13**.

83 T. Rohrlack, Low temperatures can promote cyanobacterial bloom formation by providing refuge from microbial antagonists, *AIMS Microbiol.*, 2018, **4**, 304, DOI: **10.3934/microbiol.2018.2.304**.

84 K. A. Lenz, T. R. Miller and H. Ma, Anabaenopeptins and cyanopeptolins induce systemic toxicity effects in a model organism the nematode *Caenorhabditis elegans*, *Chemosphere*, 2019, **214**, 60–69, DOI: **10.1016/j.chemosphere.2018.09.076**.

85 J. Jankowiak, T. Hattenrath-Lehmann, B. J. Kramer, M. Ladds and C. J. Gobler, Deciphering the effects of nitrogen, phosphorus, and temperature on cyanobacterial bloom intensification, diversity, and toxicity in western Lake Erie, *Limnol. Oceanogr.*, 2019, **64**, 1347–1370, DOI: **10.1002/lno.11120**.

86 Lake Diefenbaker Irrigation Projects, **https://diefenbakerirrigation.ca/**, accessed December 2021.

87 Y. Dibike, A. Muhammad, R. R. Shrestha, C. Spence, B. Bonsal, L. de Rham, J. Rowley, G. Evenson and T. Stadnyk, Application of dynamic contributing area for modelling the hydrologic response of the Assiniboine River basin to a changing climate, *J. Great Lake. Res.*, 2021, **47**, 663–676, DOI: **10.1016/j.jglr.2020.10.010**.